ELSEVIER

www.elsevier.nl/locate/carres

Carbohydrate Research 322 (1999) 228–246

CARBOHYDRATE RESEARCH

Band-flip and kink as novel structural motifs in α-(1→4)-D-glucose oligosaccharides. Crystal structures of cyclodeca- and cyclotetradecaamylose

Joël Jacob [a], Katrin Geβler [a], Daniel Hoffmann [b], Haruyo Sanbe [c], Kyoko Koizumi [c], Steven M. Smith [d], Takeshi Takaha [e], Wolfram Saenger [a,*]

[a] *Institut für Kristallographie, Freie Universität Berlin, Takustraße 6, D-14195 Berlin, Germany*
[b] *GMD-SCAI, Schloß Birlinghoven, D-53754 Sankt-Augustin, Germany*
[c] *School of Pharmaceutical Sciences, Mukogawa Women's University, 11–68 Koshien, Kyuban-cho, Nishinomiya, Hyogo 663, Japan*
[d] *Institute of Cell and Molecular Biology, University of Edinburgh, The King's Buildings, Mayfield Road, Edinburgh EH9 3JH, UK*
[e] *Biochemical Research Laboratory, Ezaki Glico Co., Ltd., 4-5-6 Utajima, Nishiyodogowa, Osaka 555, Japan*

Received 24 June 1999; accepted 30 July 1999

Abstract

Cycloamyloses (CAs) with 10 and 14 glucose units (cyclodeca- and cyclotetradecaamylose, or ι-cyclodextrin and ε-cyclodextrin, respectively) crystallize as 23.5 and 29.7 hydrates, respectively. Both crystals belong to the monoclinic space group *C*2, with half molecules in the asymmetric unit, the other halves being related to the first by crystallographic twofold axes. NMR and X-ray analyses show that in CA10 and CA14, two diametrically opposed glucoses are flipped ~180°, leading to elliptical structures with narrow, slit-like cavities. In both molecules, the flipped glucoses are stabilized in orientation by intramolecular three-centered hydrogen bonds with O-3(n)–H as donor, namely O-3(n)–H···O-6($n+1$)B and O-3(n)–H···O-5($n+1$). The other glucoses are stabilized by O-2(n)···O-3($n-1$) hydrogen bonds (as observed in the smaller α-, β- and γ-cyclodextrins) except at two kinks where these distances are long (3.98 and 3.39 Å, respectively). The geometry at the flip site, unusual for α-D-glucoses oligosaccharides, is similar to the one observed in the crystal structure of β-D-cellotetraose (structural model for cellulose II). In both molecules, conformations are unstrained with glucoses in $^4C_1$ form. Due to their conformational pecularities, CA10 and CA14 crystal structures combine in their crystal lattice the two common packing motifs characteristic of the smaller cyclodextrins, namely parallel channels with intermolecular contacts in herringbone arrangement. Since ^{13}C NMR chemical shifts observed with CAs and amylose in solution and solid state are similar, we anticipate the presence of band-flips and kinks in the polymer. As demonstrated by computer simulations, the band-flip's novel structural motif occurs in (cyclo)amylose to relieve steric strain.

Keywords: Cyclodecaamylose; Cyclotetradecaamylose; X-ray structure; Band-flip; Kink

1. Introduction

X-ray and neutron diffraction studies of a large number of crystalline cyclodextrin (CD) complexes and hydrates of α-, β- and γ-CDs

* Corresponding author. Tel.: +49-30-838-3412; fax: +49-30-838-6702.
E-mail address: saenger@chemie.fu.berlin.de (W. Saenger)

0008-6215/99/$ - see front matter
PII: S0008-6215(99)00216-5

have revealed geometrical characteristics of the host–guest interaction as well as conformational properties of the macrocycles [1–3]. The shapes of the CDs resemble truncated cones in which all glucoses adopt the $^4C_1$-chair conformation and are in the same syn orientation with O-2 and O-3 hydroxyls on the wide edge of the cone, and the O-6 hydroxyls on the narrow edge so that CDs are hydrophilic at the outside. By contrast, the central cavity is hydrophobic as it is coated with C-3–H, C-5–H, C-6–H_2 and the glycosidic O-4 and endocyclic O-5 oxygen atoms. The main degree of structural freedom is in the orientation of the C-6–O-6 hydroxyl groups. Preferentially, they adopt the (−)gauche conformation (O-5–C-5–C-6–O-6: $\sim -60°$) so that the O-6 is pointing 'away' from the center of the cavity. If O-6 is hydrogen bonded to a guest molecule, the (+)gauche conformation may be observed (O-5–C-5–C-6–O-6: $\sim 60°$), but the trans conformation (O-5–C-5–C-6–O-6: $\sim 180°$) has never been found thus far.

The cone structure of α-, β- and γ-CD is mainly stabilized via intramolecular O-2(n)···O-3($n-1$) hydrogen bonds between adjacent glucoses. The diameter of the cavity gradually increases with the number of glucose units (4.7–5.2, 6.0–6.4 and 7.5–8.3 Å for α-, β- and γ-CD, respectively), while the height of the torus, determined by the length of the D-glucose, is constant (~ 8 Å). The increase of the annulus size is accompanied by a reduction of curvature associated with compression of the O-2(n)···O-3($n-1$) hydrogen-bonding distances, from 3.0 Å for α-CD to 2.82 Å for γ-CD. The macrocyclic geometry is determined by nearly planar polygons formed by the glycosidic O-4 oxygens. Associated with the size of the CD, the sides and the internal angles of the polygons increase, i.e., the O-4(n)···O-4($n-1$) distances are 4.27, 4.37 and 4.50 Å, the O-4(n)···O-4($n-1$)···O-4($n-2$) angles are 120, 128 and 135°.

Interestingly, for CA9 (δ-CD, cyclononaamylose) [4], the O4 atoms describe an ellipse distorted in the shape of a boat, with outer diameters of ~ 10 and ~ 14.7 Å. As observed for CA6 to CA8, the O-2, O-3 hydroxyls are syn arranged in circular form and located at the wider 'deck' side of the boat shape. They are hydrogen bonded except for two glucoses where the O-2(n)···O-3($n-1$) hydrogen bonds are long (> 3.2 Å) due to steric strain [5]. The O-6 hydroxyls are on the 'hull' side and point towards the central cavity, which is considerably narrowed. Since only small amounts of CA9 are available, nothing is known about its inclusion properties.

With cyclodextrin glycosyltransferase acting on synthetic amylose, CAs with dp < 16 may be obtained and, employing disproportionating enzyme, it was shown recently that CAs with at least 17 and more than 100 glucoses in the ring can be produced on preparative scale and are now available for physical studies [6,7]. In the series CA10 to CA32 (except CA15 and CA19, which were not available), we were able to crystallize CA10, CA14 and CA26. In a recent preliminary communication, we have reported the X-ray crystal structures of CA10 and CA14 (cyclodeca- and cyclotetradecaamylose, respectively) [5]. In contrast to CA6 to CA8, these larger CAs are not annular in shape but elliptical with narrow, groove-like cavities because two diametrically opposed glucoses are flipped $\sim 180°$ to relieve steric strain and stabilized in this conformation by unusual three-center O-3(n)–H···O-6($n+1$)/O-5($n+1$) hydrogen bonds.

2. Experimental

Sample preparation, crystallization and structure determination.—Mixtures of larger CAs were produced by the action of cyclodextrin glucanotransferase on synthetic amylose; individual CAs were purified by repeated HPLC using ODS columns with aq MeOH as solvent (2 to 5% (v/v), and characterized as reported [5]. Crystals of both CA10 and CA14 were grown from aqueous solutions using the vapor diffusion technique. Initially, the reservoir contained 10 mL of 10% PEG 400 solution. Sitting drops of 6 μL consisted of 3 μL of reservoir solution and 3 μL of 2% (w/v) CA dissolved in water. The PEG concentration was gradually increased to optimize conditions. Crystals grew at 18 °C when the PEG concentration in the reservoir reached 17.5–20%.

For X-ray experiments, crystals and some mother liquor were sealed in quartz capillaries to prevent drying; space group and crystallographic data for CA10 and CA14 are given in Table 1. Besides X-ray data measured with in-house instrumentation [5], high-resolution data have been collected using synchrotron radiation at beamline X31 (DESY, EMBL-Outstation, Hamburg), $\lambda = 0.75$ Å, with a Mar Research image plate detector (radius 90 mm). Due to instrumental geometry and for accuracy, high (4.5–0.92 Å) and low (20–2.0 Å) resolution data were measured separately on the same crystal, and merged. The data were processed using the *hkl* program package [8], finally yielding 3298 ($3156 > 4\sigma$) and 4957 ($4738 > 4\sigma$) unique reflections for CA10 and CA14, respectively (Table 1).

Table 1
Crystallographic data and refinement parameters for CA10 and CA14

	CA10	CA14
Chemical formula	$(C_6H_{10}O_5)_{10}$	$(C_6H_{10}O_5)_{14}$
	$\times \cdots 23.50\ H_2O$	$\times \cdots 29.7\ H_2O$
Formula weight	2042	2803
Space group	$C2$, $Z = 2$	$C2$, $Z = 2$
Unit cell constants		
a (Å)	29.382(5)	36.813(9)
b (Å)	9.999(1)	10.133(2)
c (Å)	19.431(2)	21.307(4)
β (°)	121.39(2)	116.00(2)
Volume (Å^3)	4874	7144
Calculated density (g cm^{-3})	1.362	1.276
Wavelength (Å)	0.75	0.75
Resolution range (Å)	20–0.92	20–0.92
Unique reflections:		
all data	3298	4957
$<4\sigma F$	3156	4738
Completeness (%)	95.6	96.4
R_{sym} [a] (%)	4.1	3.2
Number of parameters	746	1044
Final R:		
for all data	0.052	0.068
for data $>4\sigma F$	0.050	0.066
wR_2:		
for all data	0.140	0.179
for data $>4\sigma F$	0.133	0.170
GooF	1.028	1.109
$\Delta(\rho)_{max} - \Delta(\rho)_{min}$ (e Å^{-3})	0.35/−0.36	0.53/−0.38

[a] $R_{sym} = \Sigma|I - \langle I \rangle|/\Sigma I$.

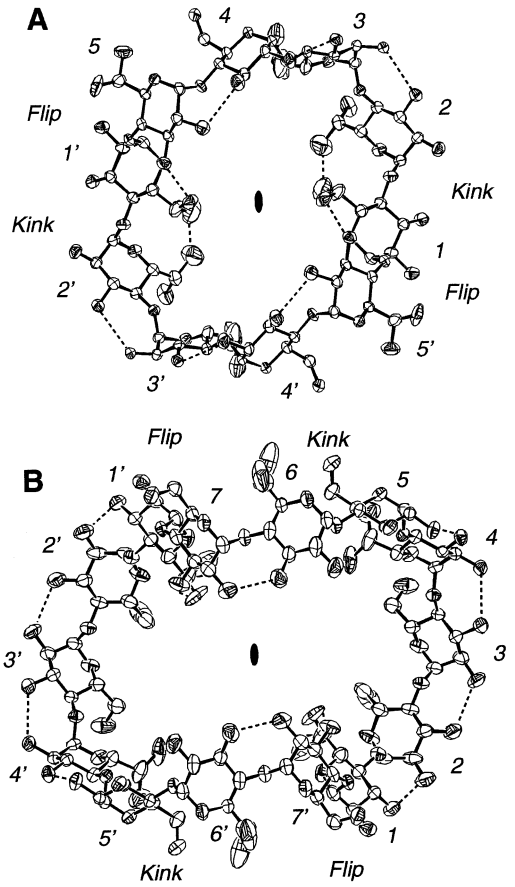

Fig. 1. Molecular structures of CA10 (A) and CA14 (B). Glucoses related by the twofold rotation symmetry are denoted with primed and unprimed numbers. Disordered O-6(n)A are in the preferred − gauche and O-6(n)B in the less favourable + gauche orientation. Hydrogen bonds indicated by dashed lines. ORTEP plot with thermal ellipsoids at 50% probability level [11].

Both crystal structures were solved by direct methods (SIR92) [9] and refined in full-matrix least-squares refinement cycles [10]; all atomic positions were treated anisotropically (Fig. 1) [11] as described [5]. Hydrogen atoms of O–H groups and water molecules could not be located, but the H-atoms of C–H groups were included in the refinement as fixed idealized isotropic contribution (d(CH) = 0.96 Å). Water positions were gradually located from a series of difference Fourier analyses, guided by inspection of the electron density maps.

Refinement of CA10 converged at an R-value of 0.050 for 3156 reflections with $F_o > 4\sigma$ (0.052 for all 3298 reflections), Table 1. The asymmetric unit contains half the CA10 molecule and 11.75 co-crystallized water molecules; three water molecules are fully occupied and 8.75 are disordered over 17 sites,

in the occupation range 0.22–0.7. All CA10 atoms are fully occupied except for the O-6 hydroxyls of glucoses G1, 2, 3 and 5, where oxygen atoms are twofold disordered with relative occupancies O-6A/O-6B at 0.48/0.52; 0.8/0.2; 0.6/0.4; 0.62/0.38, respectively.

For CA14, refinement converged at an R-value of 0.066 for 4738 reflections with $F_o > 4\sigma$ (0.068 for all 4957 reflections), Table 1. The asymmetric unit contains half the CA14 molecule and 14.85 co-crystallized water molecules; four water sites are fully occupied and 10.85 water are disordered over 30 sites in the occupation range 0.23 to 0.7. All CA14 atoms are fully occupied except for the O-6 hydroxyls of glucoses G1, G4 and G6, twofold disordered with relative occupancies O-6A/O-6B 0.6/0.4, 0.47/0.53 and 0.61/0.39, respectively.

Molecular modeling and computer simulation.—Modeling and energy minimizations on CA6 to CA10 and CA14 were carried out in vacuum using the CHARMM force field (MSI, San Diego) [12]. Hydrogens were added in calculated positions if they were not located in the X-ray structure. After 5000 minimization steps (Newton–Raphson, no cutoff, dielectric constant of one) the force-field energy converged. The solvation energy was calculated using the Solvate program [13] with two cubic grids (focusing) of side lengths 81×1.0 and 101×0.3 Å, respectively. Atomic charges and radii as provided by the CHARMM22 force field were used in the Poisson–Boltzmann calculations. The dielectric constants inside and outside the CA molecules were set to one and 78.3, respectively.

3. Results and discussion

^{13}C NMR spectra reveal structural differences.—^{13}C NMR spectra recorded from solutions of CAs with increasing numbers of glucose residues (from CA6 to CA10 and CA14) showed only six sharp signals for the six chemically different carbons of the glucose units [5,14]. This indicates that in each individual molecule, all glucoses are identical on the NMR time scale. Increasing the ring size mainly affects signals of ^{13}C-1 and ^{13}C-4 involved in the glycosidic link, while resonances of the other carbons are only slightly influenced. For CA6 to CA8, ^{13}C-1 and ^{13}C-4 signals occur at $\sim$102.4 and $\sim$81.7 ppm, respectively. For CA10 and higher homologues, shifts to $\sim$100.2 and $\sim$78.3 ppm are observed (Table 2). The distinction of two groups of ^{13}C resonances indicates the presence of two structural types, one defined by the smaller CA6 to CA8 and the other one defined by CA10 and the larger CAs. For CA9, the ^{13}C-1 and ^{13}C-4 signals are intermediate, indicating that both structural forms could occur. Since the major determinants of ^{13}C-1 and ^{13}C-4 chemical shifts are conformational features associated with rotation about the glycosidic bonds [15], the different resonances of ^{13}C-1 and ^{13}C-4 in larger CAs have to be correlated with differences in structure at C-1 and C-4 atoms, with no a priori indication about the nature of these differences.

A comparison of ^{13}C NMR chemical shifts obtained for the present CA series and previously published chemical shifts for CDs and amylose in solution is provided in Table 2. The data obtained for the smaller CA6 to CA8 are in agreement with earlier studies [14,15]. The chemical shifts observed for the larger CA10 and CA14 are in a similar range to those observed for amylose. This clearly indicates that the conformational peculiarities associated with C-1 and C-4 in CA10 and higher homologues are most probably also a

Table 2
^{13}C Chemical shifts (ppm) for (cyclo-)amyloses in solution

Material	C-1	C-4	C-3	C-2,5	C-6
α-Cyclodextrin [a]	102.2	82.1	74.1	72–73	61.3
β-Cyclodextrin [a]	102.6	81.9	73.9	72–73	61.2
CA10 [a]	99.7	78.0	73.7	71–73	61.4
CA14 [a]	100.5	78.9	73.7	72–73	61.4
α-Cyclodextrin [b]	102.2	82.1	74.2	72–73	61.4
β-Cyclodextrin [b]	102.6	81.9	73.9	72–73	61.2
CA10 [b]	99.7	78.0	73.7	72–73	61.5
CA14 [b]	100.4	78.9	73.7	72–73	61.4
α-Cyclodextrin [c]	102.6	82.4	74.5	72–73	61.7
β-Cyclodextrin [c]	103.1	82.3	74.3	72–73	61.7
Amylose [c]	100.9	78.6	74.6	72–73	61.9

[a] This work.
[b] From Ref. [14].
[c] From Ref. [15].

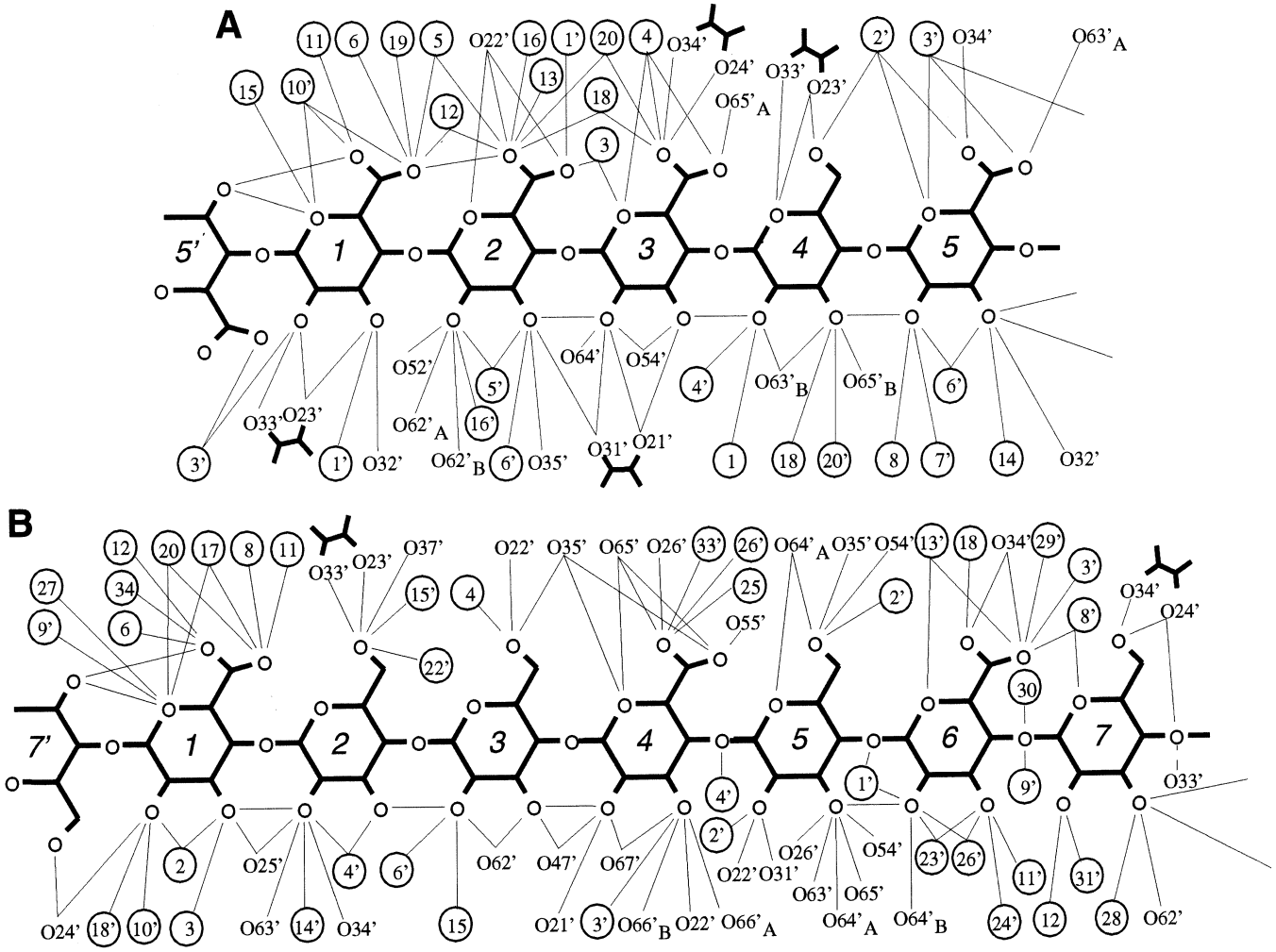

Fig. 2. Hydrogen-bonding network in CA10 (A) and CA14 (B). Thin lines indicate O···O distances < 3.4 Å, which we associate with possible hydrogen bonds as O–H hydrogens could not be located. Water oxygens are only given by their numbers and depicted as spheres; glucose hydroxyl groups numbering: O-24 means oxgen atom O-2 in glucose G4; a prime (O-24′) indicates that this glucose belongs to a symmetry-related molecule. Water···water hydrogen bonds omitted for clarity. Note preferred clustering of water molecules at the band-flip sites, glucoses G1–G5′ in CA10 and G1–G7′ in CA14.

characteristic feature of natural amylose. Since polymer amylose cannot be obtained as large single crystals, no structural model at atomic resolution is available. Structural investigations of the larger CAs are thus of importance to provide insights into the conformational changes indicated by ^{13}C NMR spectroscopy.

Molecular structure and conformational analysis.—The nature of the structural differences between the smaller CA6 to CA8 and larger CAs, as already observed in ^{13}C NMR spectra, has now been elucidated by X-ray diffraction studies of CA10 and CA14.

(a) Cycloamyloses with 10 and 14 glucoses adopt the form of a butterfly. The molecular shapes of CA10 and CA14 differ significantly from those of the smaller CA6 to CA8. This is due to $\sim 180°$ flips of two diametrically opposed glucoses in the macrocycle. They disrupt the typical ring of intramolecular O-2(n)···O-3($n-1$) hydrogen bonds (see Figs. 1 and 2) and clearly divide the molecules into two halves connected at the flip sites. All glucoses in CA10 and CA14 are in the typical $^4C_1$ chair conformation and unstrained as indicated by the Cremer and Pople puckering parameters [16,17], and by geometrical data given in Table 3 [18].

In the crystal structures, CA6 to CA8 are ‘round’, doughnut-shaped and can be described as polygons defined by the O-4 glycosidic oxygens. In CA9, the macrocycle is more elliptical, deviating strongly from the ‘polygon

Table 3
Selection of geometrical data describing the conformations of CA10 and CA14

	Glucose puckering parameters [a] QT (Å)	θ_2 [b] (°)	ϕ_2 [b] (°)	Torsion angles [c] (°)		Glycosidic bond angles C-4(n)–O-4(n)–C-1($n+1$) (°)	O-4(n)···O-4($n-1$) (Å)	O-4(n)···O-4($n+1$)···O-4($n+2$) (Å)	O-2(n)···O-3($n-1$) (Å)
				ϕ	ψ				
CA10									
Glucose 1	0.570	3.77	−94.5	*76.0*	*83.5*	*117.3*	4.52	126.7	**5.54**
Glucose 2	0.556	3.05	−99.4	102.1	122.0	120.5	4.45	142.4	*3.98*
Glucose 3	0.572	7.51	142.5	94.1	99.9	115.5	4.36	141.8	2.92
Glucose 4	0.551	3.23	170.1	102.1	96.3	120.5	4.48	134.1	3.01
Glucose 5	0.581	3.17	−167.7	**83.1**	**−64.6**	**117.3**	4.63	145.9	2.85
CA14									
Glucose 1	0.557	7.02	−107.2	103.8	106.7	117.3	4.58	135.3	**5.54**
Glucose 2	0.548	1.69	140.6	105.5	112.9	118.9	4.46	138.4	2.76
Glucose 3	0.582	2.73	−108.0	110.2	135.2	117.3	4.54	140.3	2.80
Glucose 4	0.583	6.78	−113.9	96.6	104.8	115.7	4.58	142.5	2.90
Glucose 5	0.562	3.96	−62.1	*92.7*	*91.4*	*116.3*	4.45	141.2	2.89
Glucose 6	0.551	5.30	−140.0	100.8	103.6	116.4	4.58	131.6	*3.39*
Glucose 7	0.565	3.07	−52.0	**82.0**	**−68.2**	**118.7**	4.61	138.8	2.84
Sucrose [d]	0.556	5.2	183.7						

[a] Cremer and Pople parameters [16] calculated with the program PARST [17].
[b] Spherical polar angles.
[c] According IUPAC rules [18], ϕ = O-5($n+1$)–C-1($n+1$)–O-4(n)–C-4(n) and ψ = C-1($n+1$)–O-4(n)–C-4(n)–C-3(n).
[d] Taken from Ref. [16]. Parameters determined by flip and kink sites are given in bold and italic figures, respectively.

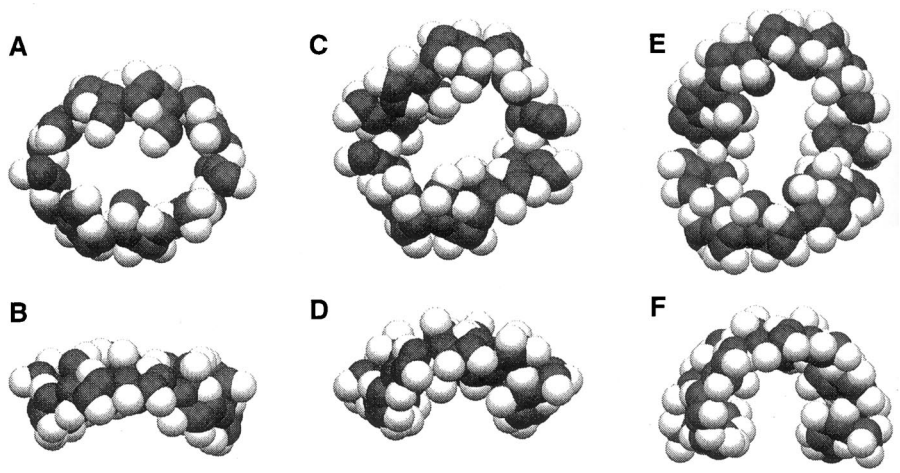

Fig. 3. Space-filling plots of CA9 (A, B), CA10 (C, D) and CA14 (E, F) in top and side views. The Figure was generated using SETOR [19]. Atomic coordinates of CA9 were kindly provided by Professor T. Fujiwara [4], C grey, and O white.

model' [4]. Moreover, this molecule is not planar but slightly bent, giving rise to a boat-shaped structure (Fig. 3(A) and (B)) [19]. In CA10 and CA14, the deviations are even stronger, and the central cavities are no longer open and round as observed for the smaller homologues but are slit-like (Fig. 3(C–F)). Both molecules have a similar structure and can be described as butterfly shaped with the wings formed by CD-like structures and the conformational flip located at the body.

To further characterize the molecular shape of the butterfly-shaped CA10 and CA14 molecules, the geometries of the 'wing' seg-

Table 4
Structural parameters of CA6 to CA8 hydrates, and the cyclodextrin-like 'wing' fragments of CA10 and CA14

		CA6 [a]	CA7 [b]	CA8 [c]	CA9 [d]	CA10 [e]	CA14 [e]
Torsion angle ϕ [f]	Average	109.2	109.8	108.9	112.1	99.4	103.4
	Min.	102.0	102.3	103.6	88.4	94.1	96.6
	Max.	114.9	118.6	123.2	138.3	102.1	110.2
Torsion angle ψ [f]	Average	128.8	127.6	127.1	124.7	106.1	112.6
	Min.	115.1	114.2	111.9	97.6	96.3	103.6
	Max.	148.7	140.4	138.5	144.5	122.3	135.2
O-4(n)···O-4($n+1$)···O-4($n+2$) angles	Average	119.9	128.3	134.9	136.6	138.2	138.2
	Min.	116.9	125.2	133.5	126.8	126.7	131.6
	Max.	122.3	132.5	136.9	149.9	145.9	142.5
O-4(n)···O-4($n+1$) distances	Average	4.235	4.385	4.502	4.489	4.488	4.540
	Min.	4.158	4.267	4.433	4.262	4.360	4.450
	Max.	4.298	4.499	4.592	4.734	4.630	4.610
O-2(n)···O-3($n-1$) distances	Average	2.981	2.884	2.823	2.906	2.927	2.830
	Min.	2.902	2.801	2.765	2.741	2.850	2.760
	Max.	3.150	2.978	2.911	3.234	3.010	2.900
C-1(n)–O-4($n-1$)–C-4($n-1$) angles	Average	118.7	118.7	116.8	116.3	118.2	117.2
	Min.	117.6	117.4	115.6	114.2	115.5	115.7
	Max.	119.6	119.8	117.7	118.9	120.5	118.9

[a] α-Cyclodextrin···7.52 H_2O [20].
[b] β-Cyclodextrin···11 H_2O [21,22].
[c] γ-Cyclodextrin···14 H_2O [23].
[d] δ-Cyclodextrin···13 H_2O [4].
[e] Only glucoses in cyclodextrin-like arrangement have been included, CA10: only three values (G2–G3–G4–G5), CA14: only five values (G1–G2–G3–G4 and G5–G6), flips and kinks have been omitted.
[f] For definition, see footnote (c) in Table 3.

ments are compared with CA6 to CA9 (Table 4) [20–23]. To make this comparison reliable, only structural parameters of CA6 7.52 hydrate (and not of the hexahydrates with distorted macrocycle) [24,25] are considered. The glycosidic ϕ and ψ torsion angles are not strongly affected with increasing ring size. Comparison of the average O-4(n)···O-4($n+1$)···O-4($n+2$) angles, O-4(n)···O-4($n+1$) distances and glycosidic angles C-1(n)–O-4($n-1$)–C-4($n-1$) shows that the wings of CA10 and CA14 have a geometry comparable to CA8 with a wider curvature than the smaller CAs. As discussed below, this may have consequences regarding the possibility of inclusion complex formation with these two larger CAs.

The average O-2(n)···O-3($n-1$) distances observed for CA7, CA8, CA10 and CA14 indicate that the hydrogen-bonding strengths within CA10 and CA14 wings are similar. In CA7, neutron diffraction studies have revealed the presence of disordered flip-flop hydrogen bonds involving O-2 and O-3 hydroxyls in dynamic equilibrium [21,22]. These flip-flop bonds are confined to CA7 and probably CA8 due to ideal interglucose geometry, with O-2(n)···O-3($n-1$) distances in a narrow range (Table 4), 2.801–2.978 Å (average = 2.884 Å) in CA7 and 2.765–2.911 Å (average = 2.823 Å) in CA8, i.e., they are energetically nearly equivalent. Since the interglucose geometry is comparable in CA10 and in CA14, with O-2(n)···O-3($n-1$) distances in the range 2.850–3.010 Å (average = 2.927 Å) and 2.760–2.900 Å (average = 2.830 Å) in CA10 and CA14, respectively, we assume that such a flip-flop disorder could also contribute to the conformational stability in the 'wing' fragments of these two larger CA. This assumption is supported by two findings: (1) in spite of the available high-resolution data, no hydrogens of the hydroxyl groups could be located in the difference electron density maps, probably because their positions are only half occupied (as observed in crystal structures of CA7 and CA8); (2) as determined experimentally, CA11, CA12 and CA13 are about 20 times more soluble than CA10 and CA14 and crystallization has not yet been successful. This may be compared with CDs where CA7 is ~10-fold less soluble than CA6 and CA8 and crystallizes more easily, probably because its structure is more rigidly confined; these observations suggest that CA10 and CA14 may also be stabilized by flip-flop hydrogen bonds, explaining their relative rigidity and lower solubility compared with CA11 to CA13. Because CA11 and CA13 do not have inherent twofold symmetry, diametrically opposed glucose flips are not possible and consequently, the molecular geometries may not allow such stabilization of molecular conformation.

(b) Band-flips and kinks are novel structural features in CA10 and higher homologues. CA10 and CA14 differ from the smaller CDs by the introduction of a novel structural motif giving rise to the typical macromolecular shape described above: two diametrically opposed glucoses are ~180° flipped, disrupting the continuous ring of intramolecular O-2(n)···O-3($n-1$) hydrogen bonds. In both molecules, the flipped glucose is stabilized in orientation by intramolecular three-centered hydrogen bonds [26] with O-3(n)–H as donor, namely O-3(n)–H···O-6($n+1$)B and O-3(n)–H···O-5($n+1$) (Fig. 4(A) and (B)) [27,28]. This interaction is unusual for α-D-glucose oligosaccharides but is comparable to the one observed in the crystal structure of β-D-cellotetraose (Fig. 4(C)) [27], a structural model for cellulose II (Table 5). The major difference between both systems is that in CA, the O-3(n)···O-5($n+1$) and the O-3(n)···O-6($n+1$)B hydrogen bonds are respectively the minor (longer) and major (shorter) components of the three-center hydrogen bond donated by O3–H, while in β-cellotetraose, the reverse is observed, which we associate with the different configurations at the glycosidic links.

The flips in CA10 and CA14 are best described by ϕ, ψ torsion angles [18]. For glucoses hydrogen bonded O-2(n)···O-3($n-1$), as in CDs, these angles are in the expected range: ϕ (94–102°), ψ (96–122°) in CA10 and ϕ (97–110°), ψ (104–135°) in CA14 (Table 3). However for the flipped glucoses, the glycosidic torsion angles ϕ and ψ are 83 and −65° for G5′–G1 in CA10 and 82 and −68° for G7′–G1 in CA14, respectively (see Table 3).

The conserved geometry of the flip in both molecules is accompanied by significant con-

formational differences along the amylose chains. In CA10, the flip occurring between glucoses G5′ and G1 is directly followed by a kink. It increases the O-2(2)···O-3(1) distance to 3.98 Å, too long for a hydrogen bond, and the orientation of glucose G2 is maintained by an unusual O-6(1)A···O-6(2)B hydrogen bond of 3.08 Å, see Fig. 4(A). The C-6–O-6 groups of these glucoses G1 and G2 are in the usual (−)gauche orientation; they point toward the center of the molecule and delimit the narrowest access to the slit-like cavity. Glucoses G2 to G5 are in CD-like arrangement and form the 'wings' of the butterfly-shaped molecule. In CA14, a kink is also present but does not, as in CA10, directly follow the flip. The next five glucoses (G1–G5) are O-2(n)···O-3($n-1$) hydrogen bonded as in CD-like structures, and the kink occurs downstream between glucoses G5 and G6. However, the O-2(6)···O-3(5) distance of 3.39 Å can be considered as long (weak) hydrogen bond stabilizing the orientations of glucoses G5 and G6. The following glucose (G7) preceding the flip again forms a normal O-2(7)···O-3(6) hydrogen bond. The O-2 and O-3 hydroxyls of these two glucoses (G6 and G7) point toward the center of cavity and delimit its width. Conse-

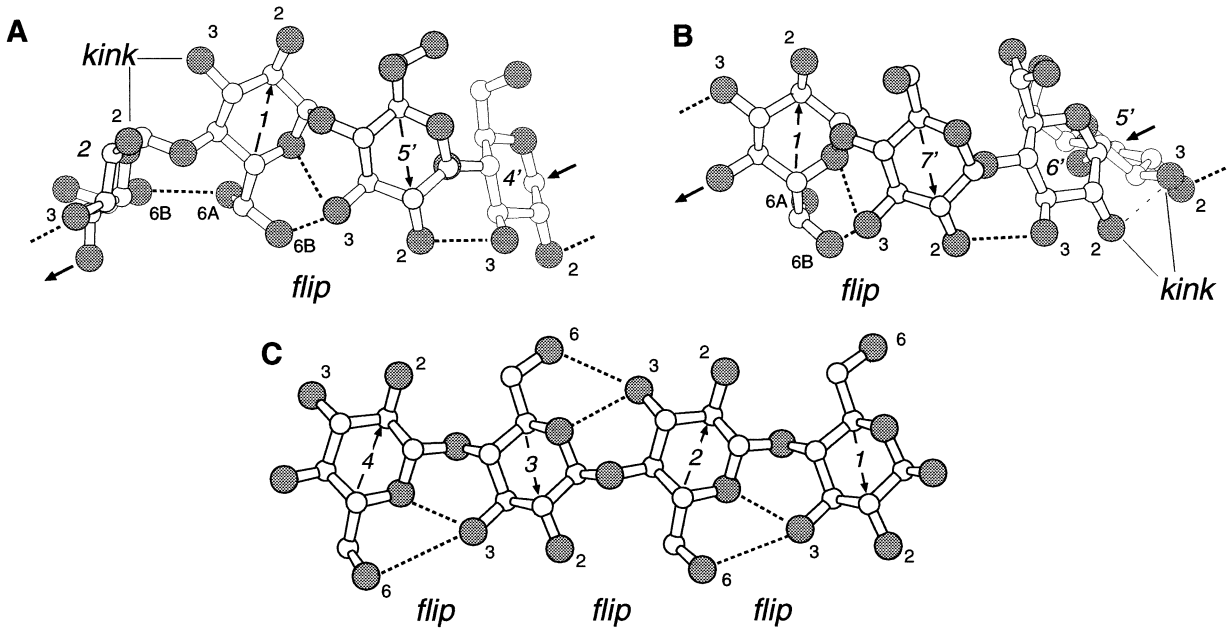

Fig. 4. Kink and band-flip sites in CA10 (A) and CA14 (B) viewed from the centre of the molecules. O-2, O-3 and O-6 (grey) atoms are numbered. Arrows in the centers of the glucose residues indicate orientations of glucoses at the band-flip sites. Thick arrows at O-4 and C-1 atoms at both ends of the fragments delineate the course of the CA chains. (C) Molecular structure of β-D-cellotetraose [27]. Figures drawn with MOLSCRIPT [28].

Table 5
Three-center hydrogen bonds at the flip sites in CA10, CA14 and in β-D-cellotetraose

	O-3(n)···O-5($n-1$)		O-3(n)···O-6($n-1$)	
	Hydrogen bond	Distance (Å)	Hydrogen bond	Distance (Å)
CA10	O-35···O-51′ [a]	3.20	O-35···O-61′B	2.77
CA14	O-37···O-51′	3.33	O-37···O-61′B	3.00
β-D-Cellotetraose: [b]				
Molecule A	O-3(n)···O-5($n-1$)	2.84	O-3(n)···O-6($n-1$)	3.32
Molecule B		2.91		3.09

[a] The primed number indicate that the glucose belongs to the symmetry-related second half of the molecule.
[b] Only average distances for the two β-D-cellotetraose molecules within the asymmetric unit are given.

Table 6
Energetics per glucose residue of cycloamyloses with increasing glucose numbers (CA6 to CA10 and CA14) [a]

	E_{tot}	E_{ff}	E_{elec}	E_{vdw}	E_{bond}	E_{angle}	E_{tors}	E_{solv}
CA6	−7.42	9.61	−11.3	−5.57	0.413	3.43	22.6	−17.0
CA7	−7.68	7.81	−13.4	−4.99	0.444	3.05	22.7	−15.5
CA8	−7.66	7.45	−13.8	−4.61	0.468	2.87	22.6	−15.1
CA9	−7.70	7.54	−13.7	−4.68	0.454	2.86	22.6	−15.2
CA10	−7.94	8.54	−11.7	−4.85	0.477	3.17	21.4	−16.5
CA14	−7.31	8.07	−13.8	−4.17	0.506	3.11	22.5	−15.4
'Unflipped' CA10	−7.56	6.24	−15.0	−4.87	0.484	3.13	22.5	−13.8

[a] All energies are given in kcal mol^{-1} per glucose monomer. E_{tot}: total energy after minimization; E_{ff}, force field [12]; E_{elec}, Coulombic; E_{vdw}, van der Waals (Lennard–Jones); E_{bond}, bond; E_{angle}, angle; E_{tors}, torsion angle and E_{solv}, solvation [13] energies.

quently, the major difference between CA10 and CA14 is that in CA10, glucose G2 following the flip is kinked and is engaged in an O-6(1)A···O-6(2)B hydrogen bond, while in CA14, all glucoses, except at the flip site, form normal, CD-like O-2(n)···O-3($n-1$) hydrogen bonds; the kink, where this bond is long and weak, is 3 glucoses away from the flip.

(c) Glucose flips have to occur to relieve steric strain. In order to better understand the reason for such a conformational difference between the doughnut-shaped CA6 to CA9 and the higher homologues, the energetics of these CA were investigated using two complementary methods. First, the X-ray crystallographic structures were energy minimized in vacuum using the CHARMM force field [12]. In a second step, the solvation energy was calculated using the Poisson–Boltzmann program SOLVATE [13]. While the total minimum energy (E_{tot}) per glucose is remarkably similar for all molecules, from −7.94 to −7.31 kcal mol^{-1} for CA10 and CA14, respectively (Table 6) the various individual energetic contributions differ more strongly, in particular the solvation (E_{solv}), Coulombic (E_{elec}), and torsion angle (E_{tors}) energies.

Interestingly, E_{elec} of CA10 is ∼2 kcal mol^{-1} per glucose residue higher than E_{elec} of CA9 and CA14, probably because CA10 is the only molecule of the series featuring a kink where the O-2(n)–H···O-3($n-1$) hydrogen bond is broken. This destabilizing factor is balanced by a ∼1 kcal mol^{-1} better solvation, and by a ∼1 kcal mol^{-1} lower torsion-angle energy, E_{tors} (Table 6). In CA10 and higher homologues, the kinks and flips are breaking the short, strong O-2(n)···O-3($n-1$) hydrogen bonds (influencing E_{elec}), and give rise to 'free' hydroxyl groups. These hydroxyls are suitable hydrogen-bond acceptors and donors and responsible for a better solvation of the molecule, compensating partly the higher force-field energy E_{ff}.

To investigate the influence of the flip and the kink on the different energetical terms, a CA10 molecule without these two new structural motifs ('unflipped-CA10') was modelled. For this purpose, the first and last glucoses of a linear amylose chain consisting of all 10 glucose units in syn orientation have been connected by a standard α-(1→4)-glycosidic bond. The constructed molecule has been energy minimized, confining ϕ and ψ torsion angles to the normal range observed in CDs. The molecule was immersed in a bath of water and subjected to molecular dynamics at 300 K for 150 ps using CHARMM [12]. From the trajectory, a conformation with a particularly low energy was selected (Fig. 5). This conformation has been investigated following the same procedure as for the series CA6 to CA10 and CA14. As expected, E_{tot} is lower (albeit, by 0.38 kcal mol^{-1}) in the naturally occurring 'flipped' CA10 structure than in the modelled 'unflipped' CA10 (Table 6). As already observed for the series CA6 to CA10 and CA14, the introduction of the kink and the flip yields a higher E_{ff}, the difference of 2.30 kcal mol^{-1} being balanced by a much better solvation (2.70 kcal mol^{-1}) of the 'flipped' structure. The conformational changes are also accompanied by more relaxed torsion-angle energy. We suspect that band-flips will also occur in all higher (cyclo-)amyloses to relieve steric strain. If this is not sufficient to stabilize the

molecule in a low-energy conformation, a kink may be introduced, further stabilizing the structure due to a much better solvation.

CA10 and CA14 crystal structures combine the channel and cage crystal packing motifs already identified in smaller cyclodextrins.—If CA6 to CA8 are crystallized either as 'empty molecules' (hydrates) or as inclusion complexes, the molecules pack in two different arrangements described as cage (brick and herringbone motifs) and channel structures according to the appearance of the cavities formed [29].

Since the butterfly-like CA10 and CA14 molecules have a comparable macromolecular conformation and both crystallize in space group *C*2, similar crystal packing is expected. As shown in Fig. 6 [30], two different packing motifs already observed in the crystal structures of smaller CD inclusion complexes can directly be identified. First, the CA10 and CA14 molecules are stacked head-to-tail along the monoclinic *b*-axes, forming infinite channels. In both crystal structures, monoclinic *b*-axes have similar lengths, namely 9.981(1) and 10.138(2) Å in CA10 and CA14, respectively, indicating that the difference in molecular size is accounted for in the dimensions of the *a*- and *c*-axes and in the monoclinic β-angle. Due to twofold screw axes parallel to the monoclinic axis, parallel stacks are offset by *b*/2. Consequently the molecules in one stack have intermolecular contacts with molecules from adjacent channels, with geometry reminiscent of the herringbone motif observed in cage-type crystal structures of smaller CDs, i.e., the CD-like parts in the wings are closed at their 'outside' by O-2, O-3 hydroxyls of molecules in adjacent stacks. Due to their conformational peculiarities, CA10 and CA14 crystal structures consequently combine in their crystal lattice the two common packing motifs characteristic of the smaller CDs, namely, (1) parallel channels with (2) intermolecular, inter-stack contacts in herringbone arrangement.

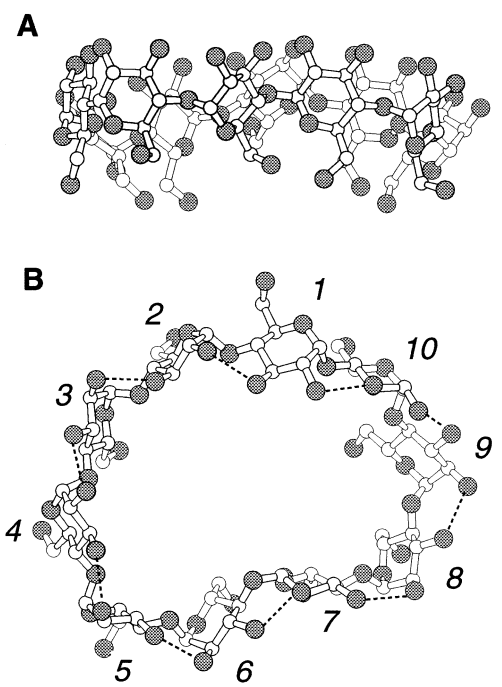

Fig. 5. Molecular structure of the modelled 'unflipped CA10' viewed from the side (A) and the top (B). O-2, O-3 and O-6 oxygen atoms are grey. Figures drawn with MOLSCRIPT [28].

Although the packing motif is similar for both crystal structures, it is obvious from Fig. 6(A–D) that CA10 and CA14 molecules have different orientations in the crystals. As shown in Fig. 6(A, C), the butterfly-like molecules give the impression of lying on the 'back' and 'front' side for CA10 and CA14, respectively. The views down the monoclinic axis (Fig. 6(B, D)), clearly indicate a different orientation of the molecules in the two crystal structures. According to the pictorial description, the butterfly would have its body parallel to the *a*-axis in CA10, while in CA14, it is parallel to the *c*-axis (see Fig. 6(B, D)).

Hydration properties.—CA10 and CA14 crystallize as 23.5 and 29.7 hydrates, respectively. In one half molecule of CA10 (the other half related to the first by crystallographic twofold symmetry), three water sites are fully occupied, the other 8.75 water molecules being disordered over 17 sites. In CA14, four water sites are fully occupied, while the other 10.85 molecules are disordered over 30 sites. The average occupancies for the disordered molecules are 0.62 and 0.37, for CA10 and CA14, respectively.

In both crystal structures, all water molecules have at least one contact < 3.4 Å to the oligosaccharides (the only exceptions are W-09 and W-17 in CA10 and W-05, W-16, W-19 and W-21 in CA14) and one or more contacts with other water molecules. The average numbers of contacts with O···O distances

<3.4 Å per water molecule are relatively high, namely 5.45 and 5.0 for CA10 and CA14, respectively. Moreover, a number of water molecules and O-6 hydroxyl groups are statistically distributed over two or more sites, with distances between these positions well below the sum of van der Waals radii of two oxygen atoms, 2.8 Å. Consequently, these sites cannot be occupied simultaneously. The heavy hydration of both molecules leads to disordered water clusters with many hydrogen-bonding contacts per water molecule and gives rise to an extended hydrogen bonding network (Figs. 2 and 7).

Fig. 8(A, C) clearly shows that in both crystal structures, water molecules are mainly situated between the wings of the butterfly-like CA10 and CA14 molecules. They preferentially have contacts to the O-6 hydroxyl groups, which are directed towards the 'inside' of the 'V' formed by the wings.

Fully occupied water molecules are mostly located in the herringbone region between CA10 and CA14 molecules (Figs. 7 and 8) where the wing-like structures are in contact. This is not surprising, since this region has a high concentration of hydroxyl groups, and its volume is not dictated by the macrocyclic shapes but by packing arrangements and requirements. The different orientations of CA10 and CA14 in the crystal lattices have an impact on their water structure. In CA10, two water sites (per asymmetric unit) are located between parallel stacks (Fig. 8(B)) while in CA14, 11 water sites are located in this region (Fig. 8(D)). Moreover, glucoses forming the inter-channel contacts in the *c*-direction have a different orientation. In CA10, these glu-

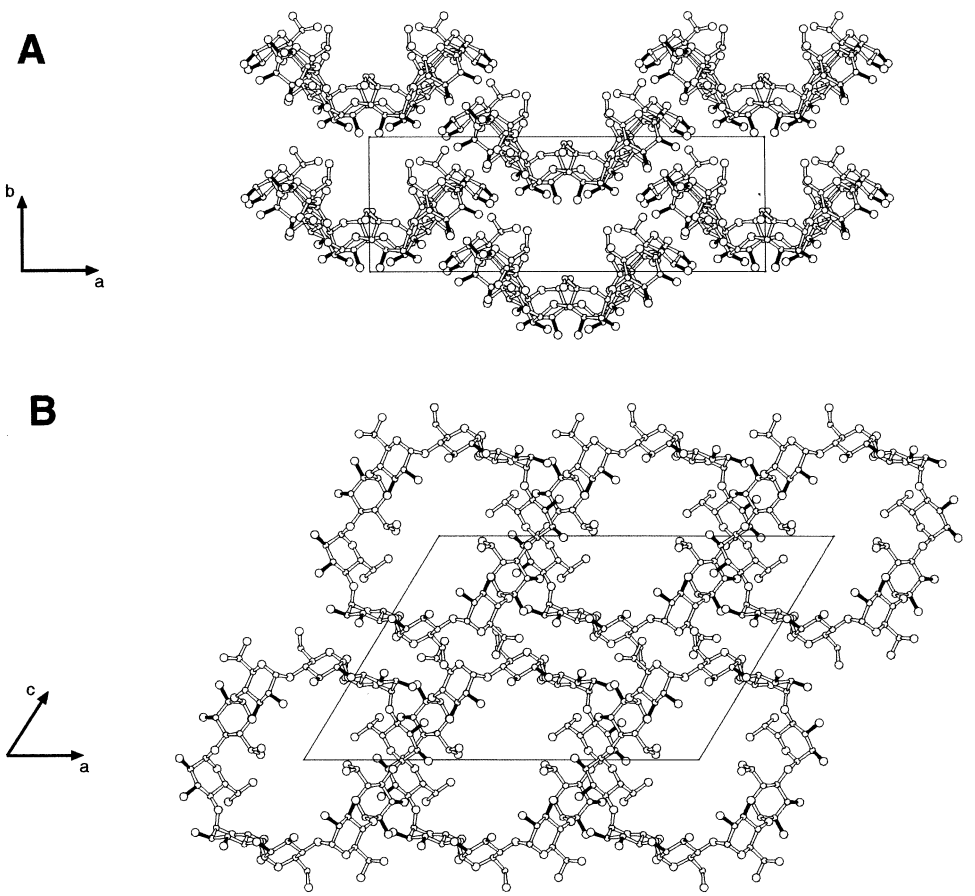

Fig. 6. Crystal packing in CA10 (A, B) and CA14 (C, D). Projection on the $a-b$ plane (along c^*) and on the $a-c$ plane (along b), respectively. Water molecules omitted for clarity. C-2(n)–O-2(n) and C-3(n)–O-3(n) bonds are filled. Note that in the butterfly-shaped molecules O-6 are 'inside' and O-2, O-3 are 'outside', clearly seen on Fig. 7(A, C) (produced with ORTEPII) [30].

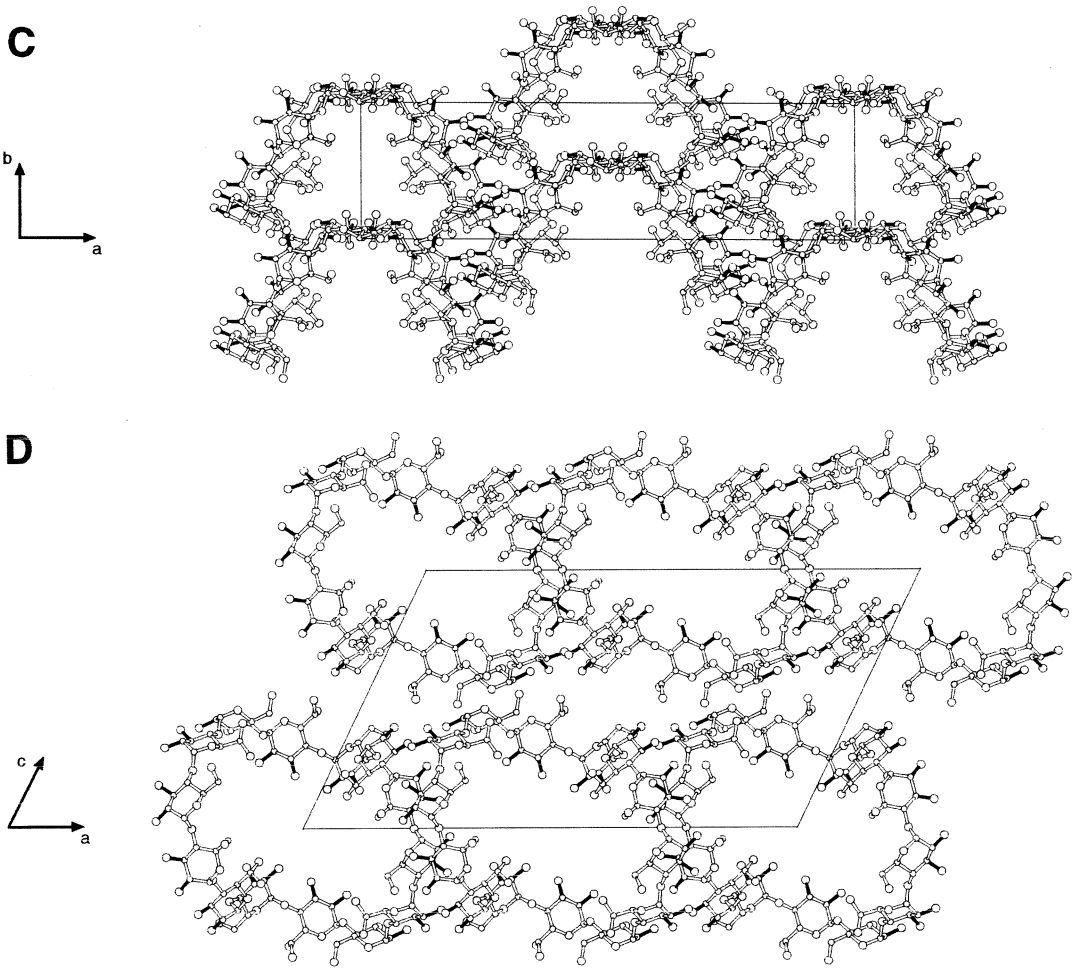

Fig. 6. (*Continued*)

coses are nearly parallel to the *b*-axis, while in CA14 they are perpendicular with the O-6 hydroxyls pointing 'away' from the center of the cavity, offering a much better geometry for hydrogen-bonded water molecules.

In the crystal structure of CDs and of the (*p*-nitrophenyl α-maltohexaoside)$_2$···Ba(I$_3$)$_2$··· 27 H_2O complex [31], a characteristic feature of the hydration pattern is the systematic formation of five-membered ring structures involving the O-2/O-3 or O-5/O-6 hydroxyl groups of the same glucose. The same hydration geometry is formed in CA10 and CA14. The five-membered ring structures occurring in CA10 and CA14 are listed in Table 7. All but one glucose (G7 in CA14) is involved in at least one five-membered ring coordination, demonstrating the relatively high stability of such a hydration structure. If this interaction involves O-5/O-6, the O-6 group can be both in + gauche and − gauche orientations.

The major structural difference in CA10 and CA14 resides in the narrowest diameter of the groove-like cavities. It is about 7 Å wide in both molecules, too short to be bridged by single water molecules, and opposed parts are related by the crystallographic twofold rotation axes (Fig. 9). In CA10, this diameter is defined by the two flipped glucoses G1 and G1′, with the twofold disordered O-6 hydroxyl groups pointing toward the center of the cavity. These two glucoses are bridged via water-mediated hydrogen bonds with eight partially occupied water sites forming two- and three-water bridges with O-6A, O-6B as bridgeheads (Fig. 9(A)), and one water site lying on the twofold crystallographic axis is linking the two bridges. Except for this water site located

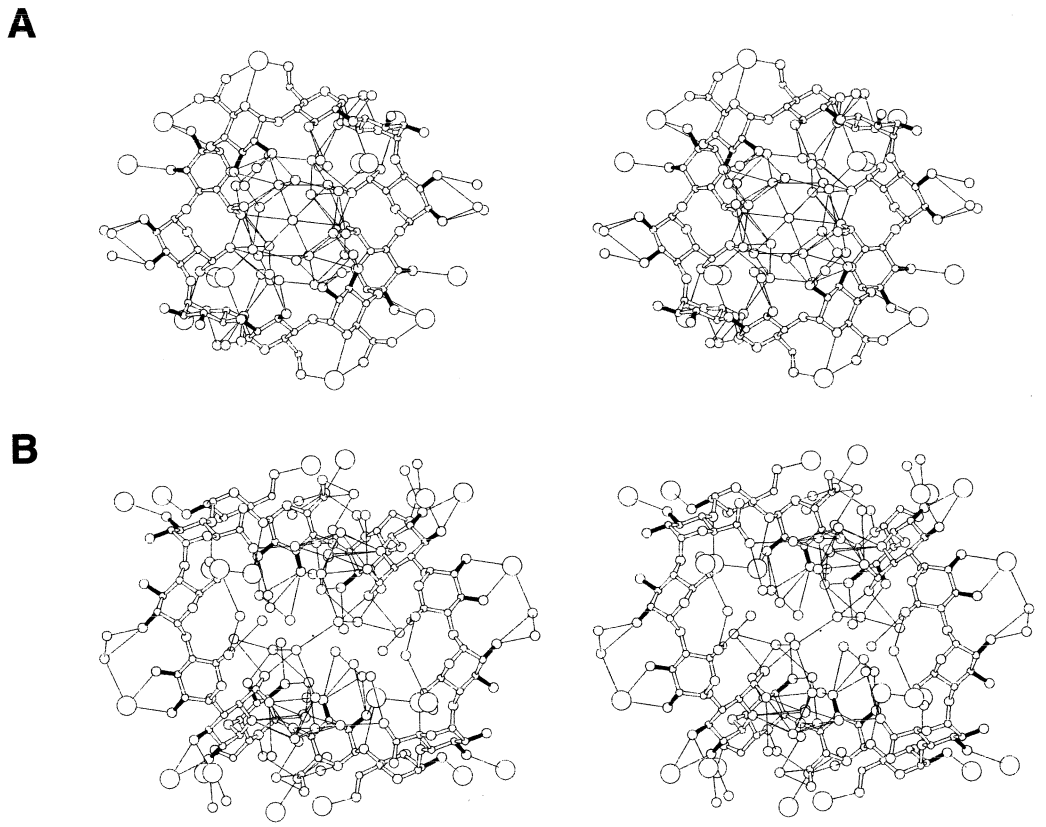

Fig. 7. CA10 (A) and CA14 (B) depicted with their respective hydration shells. All water molecules at < 3.4 Å with glucose atoms are drawn. Molecules are projected on the $a-c$ plane (along b). C-2(n)–O-2(n) and C-3(n)–O-3(n) bonds are filled, water in fully occupied sites drawn larger (produced with ORTEPII) [30].

in the center of the cavity, the hydration pattern of CA10 gives rise to a narrow 'hydrophobic hole' (see below). In CA14, the shortest distance within the cavity occurs between glucoses G6, G7 and G6′, G7′ with the O-2, O-3 hydroxyl groups pointing toward the center of the cavity. This structure is stabilized as in CA10 by water bridges involving ten partially occupied water sites organised in strings containing three and four sites, respectively (Fig. 9(B)).

Estimation of hydrophobicity shows the possibility of inclusion of guest molecules.—The inclusion-complex formation of CDs (CA6 to CA8) has been extensively studied using spectroscopic, thermodynamic and crystallographic methods [1–3]. Attention should be paid to the possible formation of such inclusion complexes with the larger homologues, since they could lead to specific and novel host–guest interactions due to their typical macromolecular forms.

A recent preliminary note reports the structure of CA10 crystallized from a 1:1 water–acetonitrile mixture [32]. This crystal had exactly the same crystallographic unit cell as CA10 crystallized from pure water (this work), and no acetonitrile molecule was found in the cavity. Since acetonitrile is known to form inclusion complexes with smaller CDs [33], it has to be concluded that inclusion properties, if present, may be different from those observed for CA6 to CA8. Since the inclusion potentials of CA6 to CA8 are directly related to the hydrophobicity and shape of their central cavities, it is of interest to obtain a visualization for the larger CAs, similar to those published for related smaller cyclic oligosaccharides [34].

In order to obtain some predictions on the hydrophobicity of the larger CAs, the energetics of hypothetical CA/Xe complexes were calculated. Xe is known to bind to smaller CDs [35,36], so that CD/Xe complexes can be

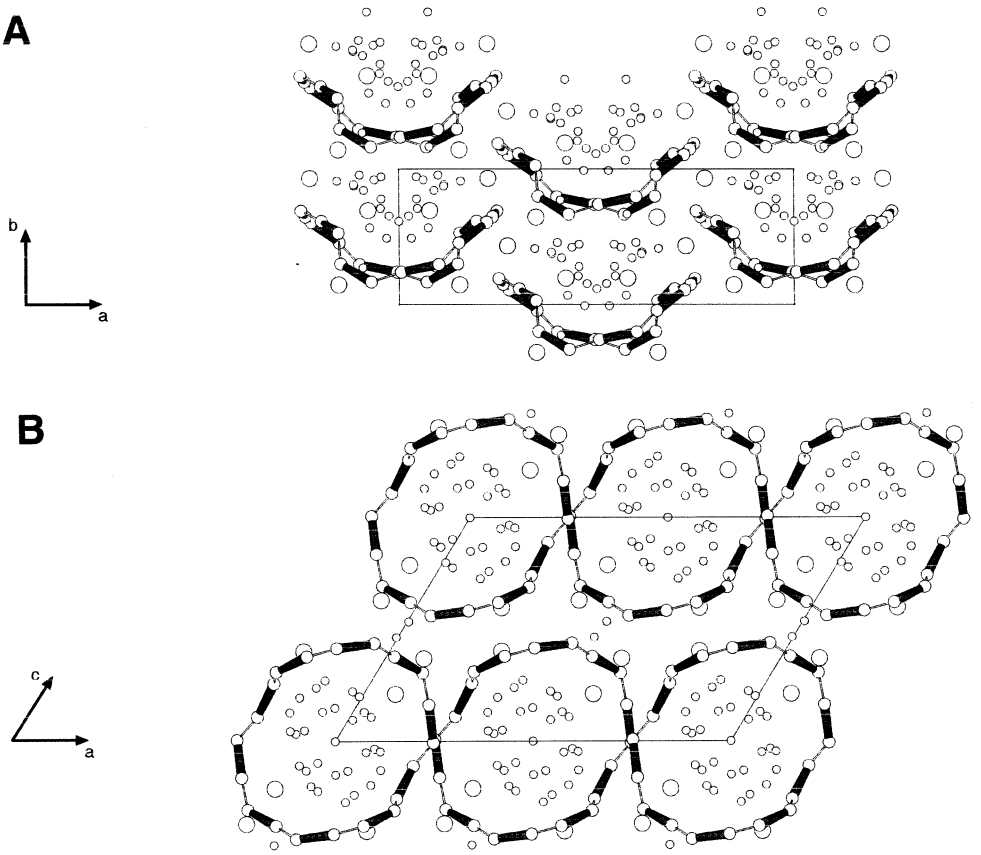

Fig. 8. Water structures in CA10 (A, B) and CA14 (C, D). Projections on the a–b plane and on the a–c plane, respectively. For clarity, glucose residues are schematically represented as thick tubes linking C-1(n) to C-4(n). Fully occupied and disordered water molecules are represented as large and small spheres respectively (produced with ORTEPII) [30].

used as references to probe the reliability of the results obtained. An energetic surface map of complexes of Xe with CA10 and CA14, respectively, was calculated by modelling the Xe atom as a spherical cavity with radius equal to the atomic radius of Xe and dielectric constant of one. Such a cavity was positioned on the van der Waals surface of the CA. For this complex, the solvation energy was calculated as described above using SOLVATE [13]. In addition, the non-polar part of the solvation energy was estimated by calculating the water-accessible surface of the complex multiplied by a surface tension of 10 cal $Å^{-2}$. The center of the cavity corresponding to Xe was then shifted to a neighboring point and the solvation energy was recalculated, etc. In this way, the Xe-accessible surface was obtained with color-coding indicating the solvation energy of the complex between Xe and the CA (not shown). The lower (higher) this energy, the more hydrophobic (hydrophilic) the surface patch is and the more (less) stable is the complex.

For CA14, the best niches for the Xe atom to bind would be the inner surfaces of the butterfly wings. They give rise to two perfect more-than-half CD molecules with five glucoses in usual O-3(n)···O-2($n-1$) hydrogen bonding contact offering similar properties because O-4, C-3–H and C-5–H coat the inner part of the wings. By contrast, the most hydrophobic region in CA10 is located between the two flipped glucoses, at the narrowest diameter of the central cavity, and on the twofold crystallographic rotation axis. Even though one has to be aware that predictions based on calculations assume that the conformations of the CAs are the same for putative complexes and for the hydrates, they provide a first insight possible inclusion into complex formation of CA10 and CA14.

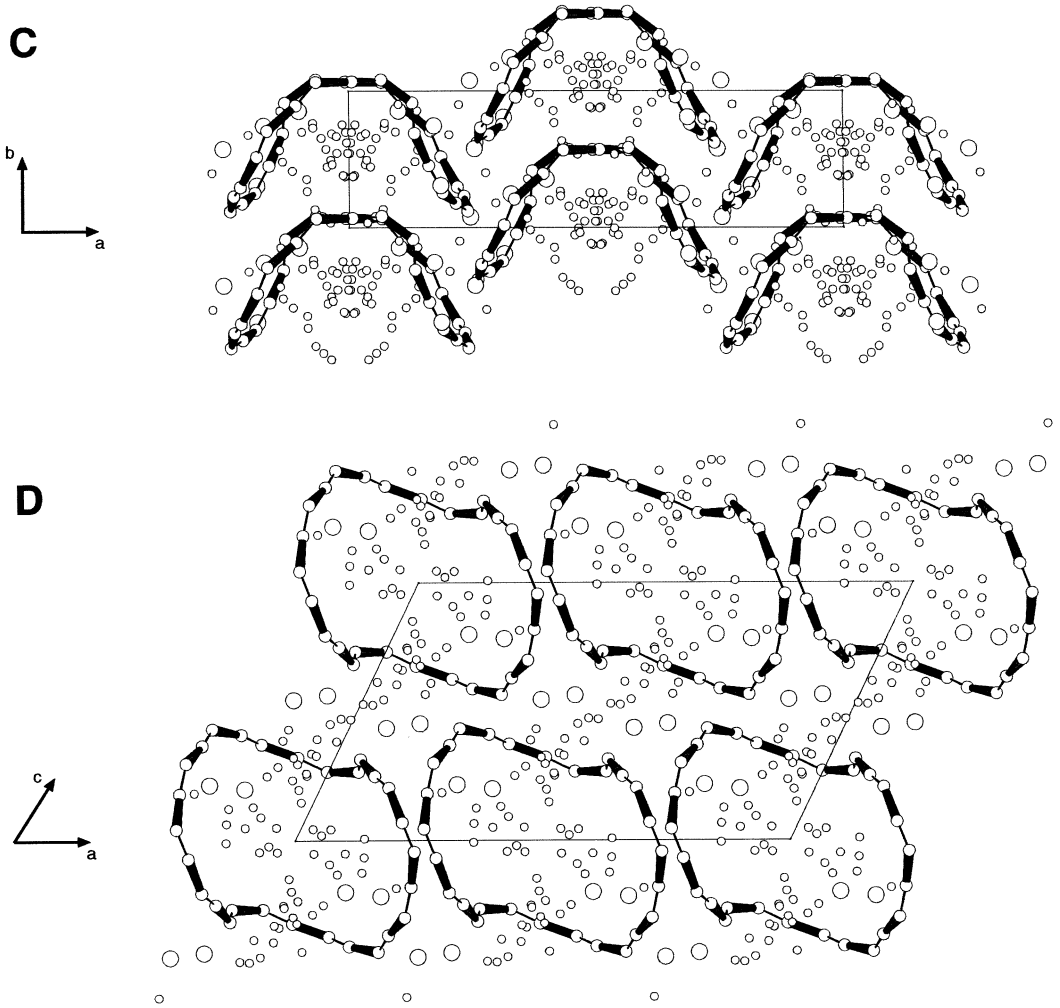

Fig. 8. (*Continued*)

4. Conclusions

Impact of the novel band-flip motif on the macromolecular structure of amylose.—Amylose, one of the two major components of starch, is a linear α-(1→4)-D-glucose polysaccharide. Depending on the source, natural starches crystallize as parallel-stranded six-fold double helices in two polymorphic forms called A and B. The sense of the helical turns is not clear, being right-handed in the older literature [37,38] and left-handed according to a more recent publication [39]. When amylose is precipitated from aqueous solution with alcohols, ketones, straight fatty acids or iodine, it forms complexes with these reagents and crystallizes in thin platelets as V amylose characterized by single-strand six-fold, left-handed helices in antiparallel arrangement [39].

Although the main folding motifs are known, there was up to now no insights into the connection between individual parallel double helices in A and B amylose or between antiparallel-oriented single strand helices in V amylose. The NMR data presented above (Table 2) indicate that the new structural motif (band-flip) occurring in large CAs determines the ^{13}C resonance of C-1 and C-4 carbons. Comparison of the chemical shifts observed with CAs and with amylose in solution and solid state clearly suggests the ubiquitous presence of the band-flip in these molecules. Connections between helices with different orientations or different forms are probably associated with band-flips. This

Table 7
Five-member ring structures formed by coordination of O-2, O-3 and O-5, O-6 hydroxyl groups in CA10 and CA14

Glucose residue	Five-membered ring via	Coordinating atom	Distances (Å)	Symmetry
CA10				
1	O-2, O-3	O-23′	2.978, 3.108	$-x+1/2, y-1/2, -z$
1	O-5, O-6A	W-10′	3.086, 3.138	$-x+1, y, -z$
1	O-5, O-6B	O-35′	3.207, 2.758	$-x+1, y, -z$
1	O-5, O-6B	W-10′	3.086, 2.902	$-x+1, y, -z$
2	O-2, O-3	W-5′	2.852, 3.378	$-x+1/2, y-1/2, -z$
2	O-5, O-6A	O-22′	2.996, 3.349	$-x+1/2, y+1/2, -z$
2	O-5, O-6B	O-22′	2.996, 3.206	$-x+1/2, y+1/2, -z$
3	O-2, O-3	O-21′	2.978, 2.938	$-x+1/2, y+1/2, -z$
3	O-2, O-3	O-54′	3.258, 3.241	$-x+1, y, -z+1$
3	O-5, O-6A	W-4	3.328, 2.743	x, y, z
3	O-5, O-6B	W-4	3.328, 2.653	x, y, z
4	O-2, O-3	O-63B′	2.964, 3.181	$x, y-1, z$
4	O-5, O-6	O-23′	3.258, 2.889	$-x+1, y, -z+1$
5	O-5, O-6B	W-6′	3.301, 3.329	$-x+1, y-1, -z$
5	O-5, O-6B	W-2′	2.956, 2.913	$-x+3/2, y+1/2, -z+1$
CA14				
1	O-2, O-3	W-2	3.023, 3.043	x, y, z
1	O-5, O-6A	W-17	3.261, 2.811	x, y, z
1	O-5, O-6A	W-20	3.269, 2.737	x, y, z
1	O-5, O-6B	O-37′	3.331, 2.977	$-x, y, -z$
2	O-2, O-3	W-4′	2.906, 2.823	$-x-1/2, y-1/2, -z$
3	O-2, O-3	O-62′	3.081, 3.249	$-x-1/2, y+1/2, -z$
4	O-2, O-3	O-67′	2.946, 3.139	$-x-1/2, y-1/2, -z$
4	O-5, O-6A	O-35′	2.909, 3.241	$x, y-1, z$
4	O-5, O-6A	O-65′	3.085, 2.991	$-x-1/2, y-1/2, -z-1$
5	O-5, O-6	O-64A′	2.980, 2.991	$-x-1/2, y+1/2, -z-1$
5–6	O-45, O-26	W-1	3.337, 2.877	x, y, z
6	O-2, O-3	W-26′	3.244, 2.947	$-x, y+1, -z$
6	O-5, O-6A	W-13′	3.289, 2.615	$-x, y-1, -z$

novel structural motif allows directional changes and avoids destabilization of the polysaccharide chain due to steric strain that would otherwise occur.

5. Supplementary material

Tables of fractional atomic coordinates of CA10 and CA14 hydrates, anisotropic displacement parameters, bond distances and bond angles (three and four pages for CA10 and CA14, respectivey); table of $F_o - F_c$ (16 pages for CA10 and 21 pages for CA14). This material is contained in many libraries on microfiche, immediately follows this article in the microfilm version of the journal, can be ordered from the ACS, and can be downloaded from the Internet; see any current masthead page for ordering information and Internet access instruction.

Acknowledgements

These studies were supported by a grant of the EU Human Capital and Mobility program to J.J., by Deutsche Forschungsgemeinschaft, Fonds der Chemischen Industrie and COMPCHEM/HLRZ at GMD-SCAI. N. Krauβ and M. Añibarro are gratefully acknowledged for assistance in data collection and helpful discussions. We thank Professor T. Fujiwara for providing atomic coordinates of CA9 and Professor K. Yamaki and her staff at Mukgawa Women's University for measuring the ^{13}C NMR spectra.

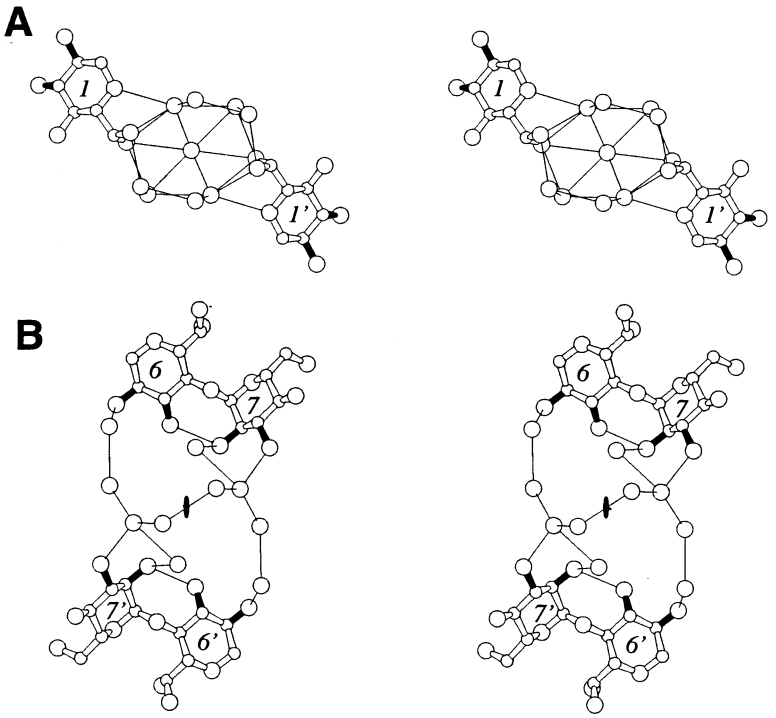

Fig. 9. Stereo view of the stabilization by water-mediated hydrogen bonding across the diameter of the groove-like cavity in CA10 (A) and CA14 (B). C-2(*n*)–O-2(*n*) and C-3(*n*)–O-3(*n*) bonds are drawn filled (produced with ORTEPII) [30].

References

[1] W. Saenger, *Angew. Chem. Int. Ed. Engl.*, 19 (1980) 344–362.
[2] W. Saenger, in J.L. Atwood, J.E.D. Davies, D.D. MacNicol (Eds.), *Inclusion Compounds*, Vol. 2, Academic Press, London, 1984, pp. 231–260.
[3] K. Harata, *Inclusion Compounds*, 5 (1991) 311–344.
[4] T. Fujiwara, S. Tanaka, S. Kobayashi, *Chem. Lett.* (1990) 739–742.
[5] J. Jacob, K. Geßler, D. Hoffmann, H. Sanbe, K. Koizumi, S. Smith, T. Takaha, W. Saenger, *Angew. Chem.*, 110 (1998) 626–629.
[6] T. Takaha, N. Yanase, H. Takata, S. Okada, S. Smith, *J. Biol. Chem.*, 271 (1996) 2902–2908.
[7] Y. Terada, M. Yanase, H. Takata, T. Takaha, S. Okada, *J. Biol. Chem.*, 272 (1997) 15279–15733.
[8] Z. Otwinowski, in L. Sawyer, N. Isaacs, S. Bailey, *Proceedings of the CCP4 Study Weekend: Data Collection and Processing*; SERC, Daresbury Laboratory, UK, 1993, pp. 56–62.
[9] A. Altomare, G. Cascarano, C. Giacovazzo, A. Guagliardi, M.C. Burla, G. Polidori, M. Camalli, *J. Appl. Cryst.*, 27 (1994) 435.
[10] G.M. Sheldrick, SHELXL93, Program for Crystal Structure Refinement, University of Göttingen, Germany, (1993).
[11] L. Zsolnai, ZORTEP, Program for Ortep Plot, University of Heidelberg, Germany (1997).
[12] B.R. Brooks, R.E. Bruccoleri, B. d. Olafson, D.J. States, S. Swaminathan, S.J. Karplus, *Comp. Chem.*, 4 (1983) 187.
[13] D. Bashford, Program Solvate, Department of Molecular Biology, The Scripps Research Institute, La Jolla, CA 92037 (1993).
[14] T. Endo, H. Nagase, H. Ueda, A. Shigihara, S. Kobayashi, T. Nagai, *Chem. Pharm. Bull.*, 45 (1997) 1856–1859.
[15] M.J. Gidley, S.M. Bociek, *J. Am. Chem. Soc.*, 110 (1988) 3820–3829.
[16] C. Cremer, J.A. Pople, *J. Am. Chem. Soc.*, 97 (1975) 1354–1358.
[17] M. Nardelli, *Comput. Chem.*, 7 (1983) 95.
[18] IUPAC, *Eur. J. Biochem.*, 131 (1983) 5–8.
[19] S.V. Evans, *J. Mol. Graph.*, 11 (1993) 134–138.
[20] K.K. Chacko, W. Saenger, *J. Am. Chem. Soc.*, 103 (1981) 1708–1715.
[21] C. Betzel, W. Saenger, B.E. Hingerty, G.M. Brown, *J. Am. Chem. Soc.*, 106 (1984) 7545–7557.
[22] T. Steiner, S.A. Mason, W. Saenger, *J. Am. Chem. Soc.*, 113 (1991) 5676–5687.
[23] K. Harata, *Bull. Chem. Soc. Jpn.*, 60 (1987) 2763–2767.
[24] B. Klar, B. Hingerty, W. Saenger, *Acta Crystallogr.*, B36 (1980) 1154–1165.
[25] K. Lindner, W. Saenger, *Acta Crystallogr.*, B38 (1982) 203–210.
[26] G.A. Jeffrey, W. Saenger, *Hydrogen Bonding in Biological Structures*, Springer Verlag, Berlin (1991).
[27] K. Geßler, N. Krauß, T. Steiner, C. Betzel, A. Sarko, W. Saenger, *J. Am. Chem. Soc.*, 117 (1995) 11397–11406.
[28] P.J. Kraulis, *J. Appl. Cryst.*, 24 (1991) 946–950.
[29] W. Saenger, *Israel J. Chem.*, 25 (1985) 43–50.
[30] C.K. Johnson, ORTEPII; Report ORNL-5138, Oak Ridge National Laboratory, Tennessee, USA (1976).
[31] W. Hinrichs, W. Saenger, *J. Am. Chem. Soc.*, 112 (1990) 2789–2796.
[32] H. Ueda, T. Endo, H. Nagase, S. Kobayashi, T. Nagai, *J. Inclusion Phenom. Mol. Recogn. Chem.*, 25 (1996) 17–20.

[33] T. Aree, J. Jacob, W. Saenger, H. Hoier, *Carbohydr. Res.*, 307 (1998) 191–197.
[34] F.W. Lichtenthaler, S. Immel, *Liebigs Ann.* (1996) 27–37.
[35] Y.-Q. Song, B.M. Goodson, R.E. Taylor, D.D. Laws, G. Navon, A. Pines, *Angew. Chem., Int. Ed. Engl.*, 36 (1997) 2368–2370.
[36] J.A. Ripmeester, C.I. Ratcliffe, J.S. Tse, *J. Chem. Soc. Faraday Trans. 1*, 84 (1988) 3731–3745.
[37] H.-C.H. Wu, A. Sarko, *Carbohydr. Res.*, 61 (1978) 27–40.
[38] A. Sarko, P. Zugenmaier, *ACS Symp. Ser.*, 141 (1980) 459.
[39] A. Imberty, H. Chanzy, S. Pérez, A. Buléon, V.J. Tran, *Mol. Biol.*, 201 (1988) 365–378.